

S.Egashira, H.S.Jin M.JSCE Faculty of Sc. & Eng., Ritsumeikan Univ.*
 O.B.Y.Liu, K.Kitayama M.JSCE River & Coastal Eng., The NEWJEC, Inc.†

1. Introduction

Bedload transport, accordingly bed feature, is closely related to flow in the vicinity of bed, and so is that of suspended load. For modeling local phenomena such as point bar and deep pool evolution in bend, local scour and fill around hydraulic structure, etc., it is quite necessary to solve the flow in 3-D. As stated in ref.(1), however, velocity near main channel bed in meandering compound flow, correspondingly pattern of secondary currents, calculated by different 3-D approach is very distinct from each other. One may infer that greater difference on simulated results of bed deformation by means of different methods of 3-D flow can be anticipated. Herein computed results of bed deformation incorporated with different approaches of 3-D flow simulation are introduced.

2. Framework of the method

Computation is conducted in boundary-fitted orthogonal curvilinear coordinates on horizontal plane (ξ, η) and a sigma-transformation in the vertical, with which unsteady and irregular boundaries are followed closely in all directions. The linked water flow prediction, based on 3-D Reynolds equations with hydrostatic pressure approximation and Boussinesq's eddy-viscosity concept, is in different turbulence closures, including 0-equation model, standard k- ϵ closure⁽²⁾ and a modified k- ϵ closure. Their constituents and computational procedure are illustrated in ref.(1). Bed variation is evaluated in terms of bedload only. 2-D form in the orthogonal curvilinear coordinate system for bed variation is expressed as:

$$\frac{\partial Z_b}{\partial t} + \frac{1}{1-\lambda} \frac{1}{g_{11}g_{22}} \left[\frac{\partial}{\partial \xi} (g_{22}q_{b\xi}) + \frac{\partial}{\partial \eta} (g_{11}q_{b\eta}) \right] = 0 \quad (1)$$

where ξ and η are the orthogonal curvilinear coordinate components; g_{11} and g_{22} are the coordinate transformation relationships; Z_b is the bed level; λ is the porosity of bed material. q_b is the volumetric bedload transport rate and is evaluated by Ashida-Michie's formula⁽³⁾. Both bottom flow direction and local bed inclination in streamwise as well as in the lateral are taken into account for the calculation of both sediment transport rate and its direction⁽⁴⁾.

The schematic view of computational flow path, 12m long and 1m wide flume with a central located sine-generated meandering main channel with width of 20cm and depth of 3cm, is shown in fig.1 of the sister paper⁽¹⁾. The following simulations start at the initial flat bed. An equilibrium sediment transportation is supposed in the following assessments. Sediment transport rate at open boundaries is calculated according to the hydraulic conditions by means of the formula of bedload transport rate. In addition, there is no lateral sediment transport across the bank. In each time step, the flow is solved first, and then sediment transport rate is calculated according to the resulting hydraulic parameters, finally eq.(1) is solved by a finite difference scheme and the advanced bed topography is obtained.

3. Result and discussion

Flow and bed evolution at the discharge of 7.15 l/s and uniform sediment bed (mean diameter=1.3mm) of the main channel are simulated by the present method. The floodplain is assumed to be fixed bed. Fig.1 shows temporal developments of secondary currents and bed evolution at section $\Phi=90^\circ$ (see fig.1 in ref.(1) for its location) computed with different turbulence closures. In the 0-equation model, eddy viscosity coefficients in horizontal plane (ν_t) and vertical direction (ν_{tz}) are evaluated as $\nu_t = \alpha u_*$ and $\nu_{tz} = \alpha_z h u_*$, respectively. Herein h =water depth, u_* =friction velocity, α and α_z are the constants.

There is a significant difference among the results of both pattern of the secondary currents and bed evolution simulated with the different turbulence closures. An approximate stable state of the bed evolution is reached soon with the standard k- ϵ turbulence closure. Actually the closure can represent isotropic turbulent flow only. For this case, due to relative shallower water depth, turbulent characteristics in vertical direction may be different from that in the horizontal. The secondary currents, shown in fig.1(b), are weakened because of the relatively larger vertical eddy viscosity (and accordingly turbulent shear stress) evaluated by the closure, which is quite important in forming bed feature. We also simulated the bed evolution with 0-equation closure of $\alpha=\alpha_z=\kappa/6$ ($\kappa=0.4$), and obtained almost a same result. With 0-equation closure of $\alpha=0.15$ and $\alpha_z=0.03$, the location and magnitude of point bar and pool can be simulated well though it results in a narrower and deeper pool as shown in fig.1(a). Multiple secondary currents and corner vortexes as shown in fig.1(c) resulted from lateral inflow and outflow of over-bank flow are reproduced with the modified k- ϵ closure.

Experimental equilibrium bed level contour and the result computed with the modified k- ϵ closure are displayed in fig.2, in which average of two measurements is used as the experimental data to exclude the influence of sand waves. The computational result mimics well the measurement in the location as well as in the magnitude of point bar and pool, and also their extent. In such

Keywords: Meandering compound channel, bed deformation, 3-D flow simulation, secondary currents, turbulence closure

* 1-1-1 Noji-higashi, Kusatsu, Shiga 525

† 20-19 Shimanouchi 1-Chome, Chuo-ku, Osaka 542

Tel.: 0775-61-2732

Tel.: 06-245-4901

Fax: 0775-61-2667

Fax: 06-245-4710

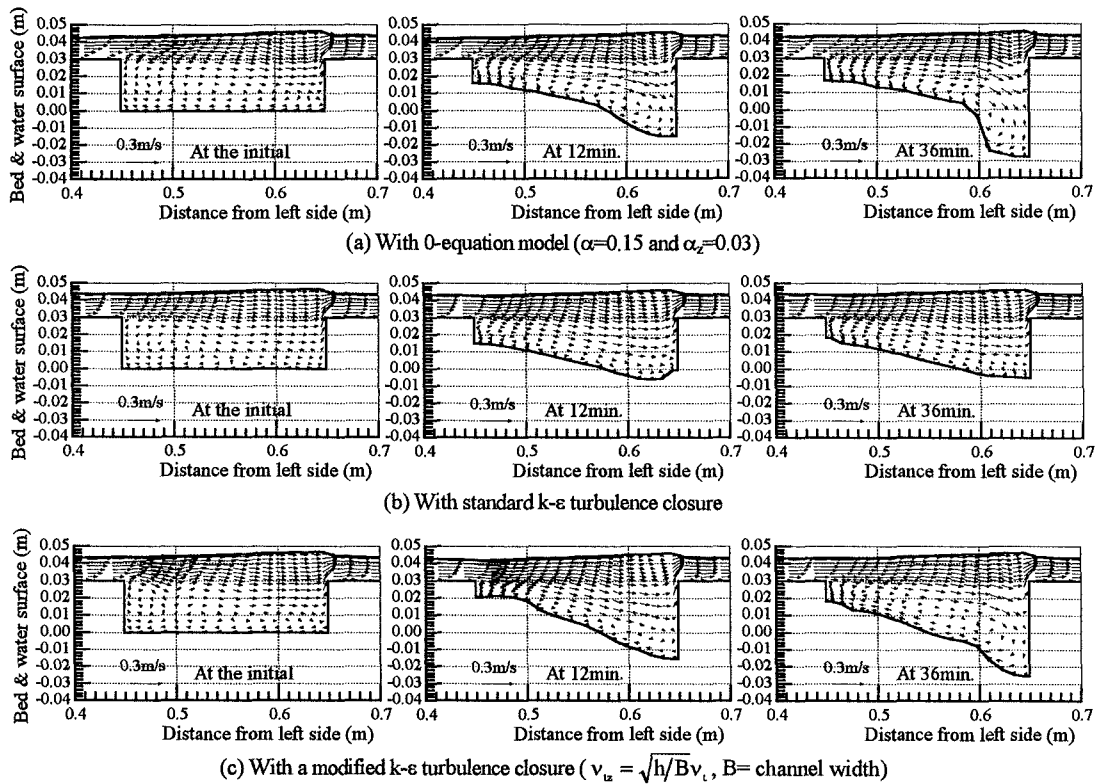
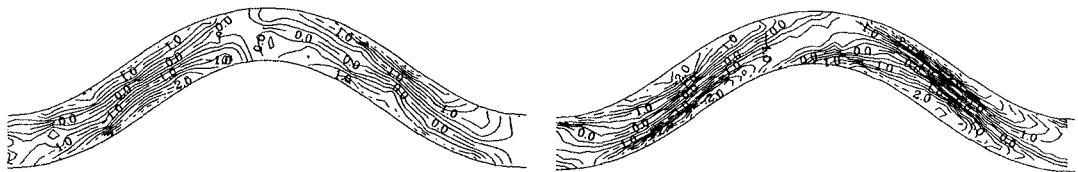


Fig.1 Secondary currents and bed evolution at section $\Phi=90^\circ$ computed with different turbulence closures

a meandering compound channel flow, scouring near the outer bank and deposition in the inner side are no longer located around bend apex as is usual in a simple meandering channel⁽⁴⁾. The point bar and pool shift more downstream, and locate around sections of $\Phi=90^\circ$ and $\Phi=270^\circ$, and their extent increases because the pattern and intensity of secondary currents as well as the locus of maximum primary flow change a lot under the interactions between main channel flow and floodplain one.



(a) Measurement

(b) Result computed with a modified k- ϵ closure

Fig.2 Equilibrium bed configuration (the contour unit: cm)

4. Conclusions

Incorporated with different 3-D approaches for water flow simulation, bed evolution in meandering compound channel is solved numerically. The development of point bar and deep pool with meandering flow path is quite distinct among the results evaluated with different approaches because they result in distinct nature on the pattern and intensity of secondary currents and so on, which take a key role in forming such a bed feature. The deformation can be reproduced reasonably by the modified k- ϵ turbulence closure. Comparing to the general bed feature in a simple cross-sectional channel, it shows that the location of pool and point bar shifts more downstream from the bend apex of main channel.

5. References

- 1) Jin, H.S., S.Egashira, B.Y.Liu and M.Sumino (1997). Evaluation of velocity near bed in meandering compound open channel flow, Proceedings of the 52nd National Conference, JSCE.
- 2) Rodi, W. (1980). *Turbulence models and their application in hydraulics*, IAHR Publication, DELFT, The Netherlands.
- 3) Ashida, K. and M.Michiue (1971). The annuals of the DPRI, Kyoto Univ., 14(B), 259-273. (in Japanese)
- 4) Liu, B.Y., H.S.Jin and S.Egashira (1997). Numerical modeling of mobile-bed evolution incorporated with 3-D flow model, Proceedings of 27th IAHR Congress, San Francisco, USA.